

## Adsorption Characteristics of Pb(II) and Cr(III) onto C-4-Methoxyphenylcalix[4]resorcinarene in Batch and Fixed Bed Column Systems

Jumina,<sup>a\*</sup> Ratnaningsih Eko Sarjono,<sup>b</sup> Brajna Paramitha,<sup>a</sup> Ika Hendaryani,<sup>a</sup> Dwi Siswanta,<sup>a</sup> Sri Juari Santosa,<sup>a</sup> Chairil Anwar,<sup>a</sup> Hardjono Sastrohamidjojo,<sup>a</sup> Keisuke Ohto<sup>c</sup> and Tatsuya Oshima<sup>d</sup>

<sup>a</sup>Department of Chemistry, Faculty of Mathematics and Natural Sciences, Gadjah Mada University, Sekip Utara, Yogyakarta 55281, Indonesia

<sup>b</sup>Department of Chemistry, Faculty of Mathematics and Natural Sciences, Indonesia Educational University, Bandung, Indonesia

<sup>c</sup>Department of Applied Chemistry, Faculty of Science and Engineering, Saga University, 1-Honjo, Saga 840-8502, Japan

<sup>d</sup>Department of Applied Chemistry, Faculty of Science and Engineering, Miyazaki University, 1-1 Gakuenkibanadai-nishi, Miyazaki 889-2192, Japan

A study on the adsorption characteristics of Pb(II) and Cr(III) cations onto C-4-methoxyphenylcalix[4]resorcinarene (CMPCR) in batch and fixed bed column systems has been conducted. CMPCR was produced by one step synthesis from resorcinol, 4-methoxybenzaldehyde, and HCl. The synthesis was carried out at 78 °C for 24 hours and afforded the adsorbent in 85.7% as a 3:2 mixture of C<sub>4v</sub>:C<sub>2v</sub> isomer. Most parameters in batch and fixed bed column systems confirm that CMPCR is a good adsorbent for Pb(II) and Cr(III), though Pb(II) adsorption was more favorable than that of Cr(III). The adsorption kinetic of Pb(II) and Cr(III) adsorptions in batch and fixed bed column systems followed a pseudo 2<sup>nd</sup> order kinetics model. The rate constant of Pb(II) was higher than that of Cr(III) in the batch system, but this result was contrary to the result obtained in a fixed bed column system. Desorption studies to recover the adsorbed Pb(II) and Cr(III) were performed sequentially with distilled water and HCl, and the results showed that the adsorption was dominated by chemisorption.

**Keywords:** Adsorption; Pb(II); Cr(III); C-4-Methoxyphenylcalix[4]resorcinarene; Batch system; Fixed bed column system.

### INTRODUCTION

Heavy metals are a common pollutant found in various industrial effluents. The strict environmental regulation on the discharge of heavy metals has led to the necessity to develop various technologies for heavy metal removal. Waste streams containing low-to-medium levels of heavy metals are often encountered in metal plating facilities, electroplating, mining operations, fertilizer, battery manufacture, dye stuffs, chemical pharmaceutical, electronic device manufactures, and many others. Most heavy metals are highly toxic and are not biodegradable; therefore, they must be removed from the polluted streams in order to meet increasingly stringent environmental quality standards.

Many methods including chemical precipitation, electro-deposition, ion-exchange, membrane separation, and

adsorption have been used to treat industrial wastes. Traditional precipitation is the most economic but is inefficient for a dilute solution. Ion exchange and reverse osmosis are generally effective, but have rather high maintenance and operation costs and are subject to fouling. Adsorption is one of the few promising alternatives for this purpose, especially using low-cost natural adsorbents such as agricultural wastes (maize cobs and husks,<sup>1</sup> ground pine cones<sup>2</sup>), charcoal,<sup>3</sup> fly ash,<sup>4</sup> zeolite,<sup>5,6</sup> and granular activated carbon.<sup>7</sup> New synthetic adsorbents have also been developed in order to generate alternative materials having different properties compared to those of natural materials.

Calix[4]resorcinarenes are a class of synthetic macromolecules having a tetramer of resorcin residues in a cyclic array and linked by a methylene bridge. The macromolecules are obtained by acid-catalyzed condensation of resorcinol with a variety of aldehydes. Calix[4]resorcinarenes

represent an interesting family of structures which exhibit the characteristic of a cavity-shaped architecture. Various studies have illustrated their application as host molecules for various guests, such as cations, anions, and molecules. The family of calix[4]resorcinarenes has also been used for various functions, namely as an additive in capillary electrophoresis,<sup>8</sup> liquid membrane,<sup>9,10</sup> extraction,<sup>9</sup> chemical sensing,<sup>11,12</sup> and High Performance Liquid Chromatography (HPLC) stationary phase. However, the use of calix[4]resorcinarenes as a heavy metal cation adsorbent is still very limited.

C-4-Methoxyphenylcalix[4]resorcinarene (CMPCR) is calix[4]resorcinarene which has eight benzene residues, eight hydroxyl groups, and four methoxy groups (Fig. 1). CMPCR was synthesized in this research through acid-catalyzed condensation of resorcinol and anisaldehyde (4-methoxybenzaldehyde). The presence of lone-pair electrons in the hydroxyl and methoxy groups, and also  $\pi$ -electrons in the aromatic residues, can be expected to exhibit characteristic affinities to heavy metal cations, especially Pb(II) and Cr(III). The former cation is considered to be a softer Pearson acid than Cr(III), which was a hard Pearson acid, while CMPCR with its hydroxyl arms and aromatic rings can form both "hard" and a "soft" ion binding sites, respectively. Thus, it was of interest to investigate the interaction of CMPCR with the two said heavy metal cations.

## RESULTS AND DISCUSSIONS

### Synthesis and Characterization of CMPCR

The synthesis of CMPCR went easy and was low-cost.

The product separated from the reaction mixture in the early minutes of reaction and gave abundant yields as light purple precipitates. The structure of CMPCR was confirmed by proton Nuclear Magnetic Resonance (<sup>1</sup>H NMR) and Fourier Transform Infrared (FTIR) spectrometers. It was interesting to note that each signal group in the <sup>1</sup>H NMR spectrum emerged as a couple of signals having a ratio of 3:2. This fact is in accordance with the findings of previous workers<sup>13-16</sup> who found that the products of condensation between resorcinol and aromatic aldehydes were only tetrameric resorcinarenes, and out of four diastereoisomeric products that could theoretically be formed, only two diastereoisomers were obtained in reality, i.e. *C*<sub>4v</sub> (*rccc*, *crown*) and *C*<sub>2v</sub> (*rect*, *chair*). The ratio of *C*<sub>4v</sub> and *C*<sub>2v</sub> isomeric products varies with the reaction time and temperature.

The interpretation of chemical shifts and the ratios of the amount of the isomers formed were determined through comparison between the proton NMR spectrum of the synthesized CMPCR and those of the *C*<sub>4v</sub> and *C*<sub>2v</sub> isomers from reactions products of benzaldehyde and resorcinol which have been separated and fully characterized by previous workers.<sup>14</sup> The *C*<sub>2v</sub> isomer was identified by two sets of single peaks for the ArOH ( $\delta_{\text{H}} = 8.40$  and  $8.46$ ) having the same integration, characteristic multiplet signal for the ArH ( $\delta_{\text{H}} = 6.11$ - $6.62$ ), a singlet methine signal ( $\delta_{\text{H}} = 5.45$ ), and a singlet peak for OCH<sub>3</sub> ( $\delta_{\text{H}} = 3.63$ ). Meanwhile, the *C*<sub>4v</sub> isomer was identified by a single peak for the ArOH ( $\delta_{\text{H}} = 8.46$ ), multiplet peaks for the ArH ( $\delta_{\text{H}} = 6.11$ - $6.62$ ), a singlet peak at 5.57 ppm of the bridging methine proton, and a singlet peak at 3.69 ppm of the methoxy protons.

Interestingly, the crown isomer (*C*<sub>4v</sub>) of CMPCR was

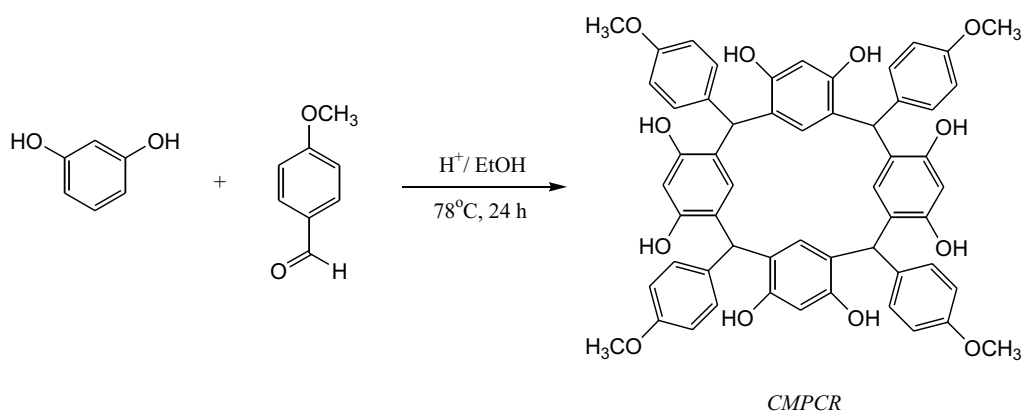


Fig. 1. Synthesis of C-4-methoxyphenylcalix[4]resorcinarene (CMPCR).

present in higher amounts compared to the chair isomer ( $C_{2v}$ ). Hydrogen bonds occurring between adjacent hydroxyl groups and the existence of staggered phenyl groups apparently stabilize the *recc* crown conformers. An extension in reaction time led to an increase in the formation of the  $C_{2v}$  isomer that was not the desired product. In order to avoid a high-cost adsorbent production, the isomeric mixture of CMPCR was used directly in the metal adsorption experiment.

The FTIR spectrum of CMPCR showed characteristic absorption at  $3419\text{ cm}^{-1}$  due to O-H stretching vibration. It is well known that absorption bands of O-H stretching vibrations, when free, appear at around  $3600\text{ cm}^{-1}$ , and a hydrogen bonding causes these bands to shift to the lower frequencies. The weak frequencies at  $2910\text{--}2837\text{ cm}^{-1}$  correspond to CH stretching frequencies. In addition, the IR spectrum also displayed a significantly intense CH bending frequency at  $1429\text{ cm}^{-1}$  and a C-O-C stretching frequency at  $1245\text{ cm}^{-1}$ .

## Batch System

### Effect of pH

The effect of pH on the adsorptions of Pb(II) and Cr(III) by CMPCR was studied in the pH range of 2.0 to 6.6 with the initial concentration of metal solution of about  $8\text{ mg/L}$ , and the results are shown in Fig. 2. The amount of Pb(II) adsorbed consistently increased by the increase of initial pH, and it reached optimum value ( $3.7\text{ }\mu\text{mol/g}$  or  $86.25\%$  in percentage) at an initial pH value of 4.07. Similar to Pb(II) adsorption, it was found that Cr(III) uptake increased from pH 2.0 to 4.59, and then decreased from pH 4.59 to 5.43. Optimum value of Cr(III) uptake ( $11.6\text{ }\mu\text{mol/g}$

or  $62.5\%$  in percentage) was reached at an initial pH of 4.59.

The fact that the amount of metal cation adsorbed at low pH was only a little apparently was caused by the occurrence of protonation of most donating groups, especially OH groups, of CMPCR. It was envisaged that the interaction between CMPCR and metal cation involved an interaction between an oxygen lone pair electrons and metal cation vacant orbitals. As the amount of  $\text{H}^+$  at low pH was sufficiently excessive in comparison to that of metal cation, most of the oxygen pair electrons perhaps did coordinate with  $\text{H}^+$  and not with metal cation. The size of  $\text{H}^+$ , which is much smaller than that of metal cation, apparently also assisted the occurrence of interaction between oxygen pair electrons of CMPCR and  $\text{H}^+$ . When the initial pH was sufficiently high (more than 4), there was only a limited amount of  $\text{H}^+$  available in the system. Accordingly, the interaction occurring in the system was dominated by the interaction between the oxygen lone pair electrons of CMPCR and the metal cation vacant orbital. This is the reason why the amount of metal adsorbed at relatively high pH values was significantly high. However, increasing initial pH to a value higher than 5.0 is not a good idea as there has been precipitation of some of metal cations.

Cr(III) is a small metal ion which is categorized as a hard acid. According to hard soft acids bases theory, this metal has a great potency to form an effective complex with CMPCR which has eight hydroxy groups and four methoxy groups that are a Pearson hard base. The results of the experiment which showed that the adsorption capacity of Cr(III) was higher than that of Pb(II) proved that the hardness of the acid and base is the key factor determining the effectiveness of the complex formation.

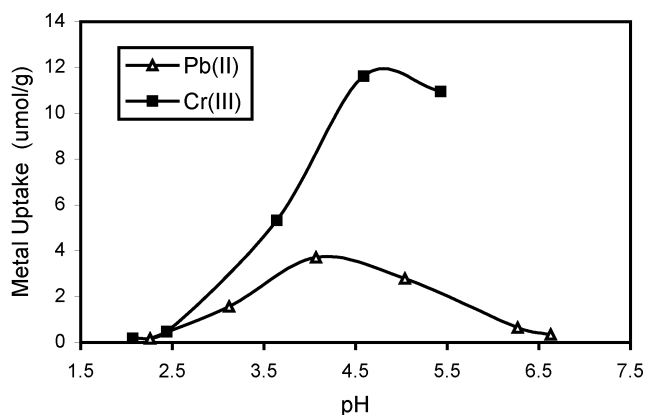


Fig. 2. Effect of pH on the adsorptions of Pb(II) and Cr(III) onto CMPCR.

### Effect of Contact Time

The result of Pb(II) and Cr(III) adsorptions at optimum pH with an increase of contact time is presented in Fig. 3. It was found that the metal uptake increased as the contact time increased. The graph indicates that the Pb(II) adsorption took place quickly in the early minutes of interaction until approximately 5 minutes giving the amount of Pb(II) adsorbed as much as  $80.46\%$  or  $3.49\text{ }\mu\text{mol/g}$ . It then increased slowly as the interaction time was extended and it reached its maximum adsorption value of  $93.48\%$  or  $4.11\text{ }\mu\text{mol/g}$  in 180 minutes. After the interaction process took place during the 180 minutes, the amount of Pb(II) adsorbed

Table 1. Kinetic parameters for Pb(II) and Cr(III) adsorptions by CMPCR

Kinetic Model	Pb(II)		Cr(III)	
	R <sup>2</sup>	k	R <sup>2</sup>	k
1 <sup>st</sup> order (Lagergren) equation $\log(q_e - q) = \log q_e - (k/2.303)t$	0.9694	$1.61 \times 10^{-5} \text{ min}^{-1}$	0.8275	$1.84 \times 10^{-5} \text{ min}^{-1}$
Pseudo 2 <sup>nd</sup> order equation $t/q = \frac{1}{2} k q_e^2 + t/q_e$	0.9999	$4.90 \times 10^{-1} \text{ g mmol}^{-1} \text{ min}^{-1}$	0.9993	$9.85 \times 10^{-2} \text{ g mmol}^{-1} \text{ min}^{-1}$
2 <sup>nd</sup> order equation $1/(q_e - q) = 1/q_e + kt$	0.9695	$4.00 \times 10^{-5} \text{ g mmol}^{-1} \text{ min}^{-1}$	0.8276	$2.00 \times 10^{-5} \text{ g mmol}^{-1} \text{ min}^{-1}$

did not change. The adsorption process at this point has reached equilibrium between the adsorbed metal ions and the free ions in solution.

A similar pattern to the previous result was obtained in Cr(III) adsorption onto CMPCR. Percentage of adsorption was dependent on the shaking time; an extension of the interaction time increased Cr(III) uptake smoothly until the uptake reached maximum value of 62% or 8.73  $\mu\text{mol/g}$  at 360 minutes (6 hours). The trend of the curve in the early minutes was almost vertical, but then it turned into almost horizontal in the following minutes, hence it could be said that the adsorption went quickly until five minutes only.

### Adsorption Kinetics

The experimental data of contact time effect on the adsorptions of Pb(II) and Cr(III) were used for kinetic modeling. The model equations used for fitting the data were: 1<sup>st</sup> order (Lagergren), pseudo 2<sup>nd</sup> order, and second order equation. The correlation coefficient (R<sup>2</sup>) resulted from a linear plot of  $\log(q_e - q)$  versus  $t$ ,  $t/q$  versus  $t$  and  $1/(q_e - q)$  ver-

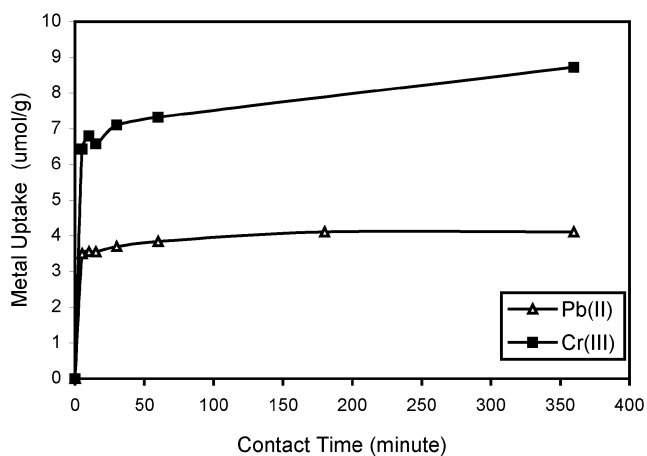


Fig. 3. Effect of contact time on the adsorptions of Pb(II) and Cr(III) onto CMPCR.

sus  $t$  (shown in Table 1). The adsorption rate constant ( $k$ ) was calculated using slope or intercept values from the equation, where  $q_e$  and  $q$  (both in  $\text{mmol g}^{-1}$ ) are the amounts of metal ion adsorbed (metal uptake) at equilibrium and at time  $t$  (min), respectively.

Based on the linear regression values, the kinetics of Pb(II) and Cr(III) adsorptions onto CMPCR could be described well by all equations, but the pseudo 2<sup>nd</sup> order equation was the best. Thus, it appeared that pseudo 2<sup>nd</sup> order was the most valid kinetics model. The Pb(II) rate constant ( $k$ ) was higher than Cr(III) rate constant for all equations, especially for the pseudo 2<sup>nd</sup> order equation where the rate constant of Pb(II) was almost five times higher than the Cr(III) rate constant. Therefore, although the amount of Pb(II) adsorbed was lower than that of Cr(III), Pb(II) adsorption onto CMPCR went faster than Cr(III) adsorption.

### Effect of Adsorbent Weight

Fig. 4 shows the effect of adsorbent weight on adsorptions of Pb(II) and Cr(III) onto CMPCR. The amount of Pb(II) adsorbed consistently increased as the adsorbent weight increased, and it reached optimum value (0.41  $\mu\text{mol}$ )

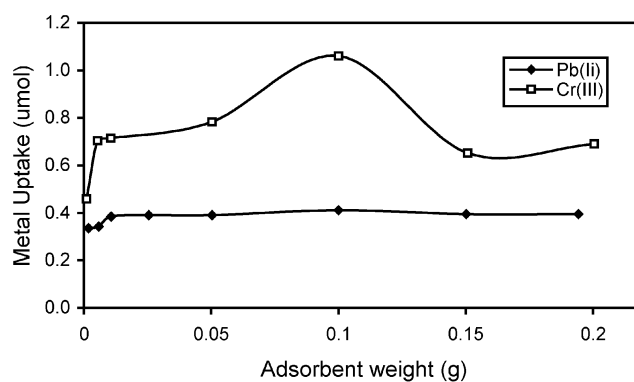


Fig. 4. Effect of adsorbent weight on the adsorptions of Pb(II) and Cr(III) onto CMPCR.

at an adsorbent weight of 0.1 g. The addition of adsorbent weight enlarged the contact surface between adsorbent and adsorbate until the exhausted condition was reached. Similar to Pb(II) adsorption, the optimum value of Cr(III) uptake (1.06  $\mu\text{mol}$ ) was reached at an adsorbent weight of 0.1 g.

### Adsorption Isotherms

The equilibrium data in the adsorption of Pb(II) and Cr(III) onto CMPCR were analyzed by using Freundlich and Langmuir isotherms, i.e.  $\log q_e = \log K + 1/n \log C_e$  and  $1/q_e = 1/(K q_0 C_e) + 1/q_0$ , respectively, where  $q_e$  is the amount adsorbed at equilibrium ( $\mu\text{mol/g}$ ),  $C_e$  is the solution concentration at equilibrium ( $\mu\text{mol/L}$ ),  $q_0$  ( $\mu\text{mol/g}$ ) is the maximum capacity of adsorption, and  $K$  is the adsorption constant. The results of linear plots of  $\log C_e$  versus  $\log q_e$  (Freundlich model) and  $1/q_e$  versus  $1/C_e$  (Langmuir model) are shown in Table 2. The  $K$  values could be calculated from the slopes and intercepts.

The data on Table 2 shows high values of correlation coefficients ( $R^2$ ) indicating linear relationships, which confirm the applicability of both adsorption isotherms. The  $R^2$  values of Pb(II) adsorption were 0.9844 and 0.9015 for Langmuir and Freundlich models, respectively, indicating that the adsorption data fitted the Langmuir model the best. On the contrary, the  $R^2$  values of Cr(III) adsorption were 0.8945 and 0.9837 for Langmuir and Freundlich models, respectively, indicating that the adsorption data fitted the Freundlich model the best. The adsorption constant ( $K$ ) of Pb(II) was higher than that of Cr(III) in the Langmuir isotherm. On the other hand, the adsorption constant ( $K$ ) of Pb(II) was lower than that of Cr(III) in the Freundlich isotherm.

The essential characteristic of the Langmuir isotherm may be expressed in terms of the dimensionless separation parameter,  $R_L$ ,<sup>17-19</sup> which is indicative of the isotherm shape that predicts whether an adsorption system is 'favourable' or 'unfavourable'.  $R_L$  is defined as:  $R_L = 1/(1 + KC_0)$ , where  $K$  is the adsorption constant, and  $C_0$  is the initial concentration of adsorbate (g/L). The adsorption is favourable when  $0 < R_L < 1$ , and the lower the value of  $R_L$  indicated a more favourable adsorption.

Variation of Gibbs free energy ( $\Delta G$ ) for the retention of adsorbate on adsorbent was determined from the adsorption constant with the aid of equation  $\Delta G = -RT \ln K$ . Some quantitative descriptions of adsorption system ( $q_0$ ,  $K$ ,  $R_L$ ,

Table 2. Estimated isotherm parameters for Pb(II) and Cr(III) adsorptions

Models	Estimated Isotherm Parameters			
	Pb(II)		Cr(III)	
	$R^2$	$k$	$R^2$	$k$
Langmuir	0.9844	152.9	0.8945	12.3
Freundlich	0.9015	485.1	0.9837	40691153.4

Table 3. Quantitative descriptions of Pb(II) and Cr(III) adsorptions on the basis of the Langmuir isotherm

Cation	$q_0$ (mmol/g)	$K$ (L/mmol)	$R_L$	$\Delta G$ (kJ/mol)	Working Range Concentration (mmol/L)
Pb(II)	$1.73 \times 10^{-1}$	152.9	0.145	-29.576	0.039-0.044
Cr(III)	$6.43 \times 10^{-3}$	12.3	0.372	-23.332	0.137-0.169

and  $\Delta G$ ) on the basis of the Langmuir isotherm model are given in Table 3.

Referring to the separation factor value ( $R_L$ ), it is obviously seen from Table 3 that CMPCR is a good adsorbent for Pb(II) and Cr(III) cations. In either case, the  $R_L$  value falls between 0 and 1, which is indicative of favourable adsorption. The  $R_L$  value also shows that the adsorption of Pb(II) was more favourable than that of Cr(III). Similarly, the negative  $\Delta G$  values confirm the spontaneous nature and feasibility of the adsorption processes, both for Pb(II) and Cr(III) adsorptions.

### Fixed Bed Column System

The percentage of metal adsorbed in a fixed bed column system is shown in Fig. 5. Pb(II) was adsorbed completely (about 100%) at some early fractions until about 14

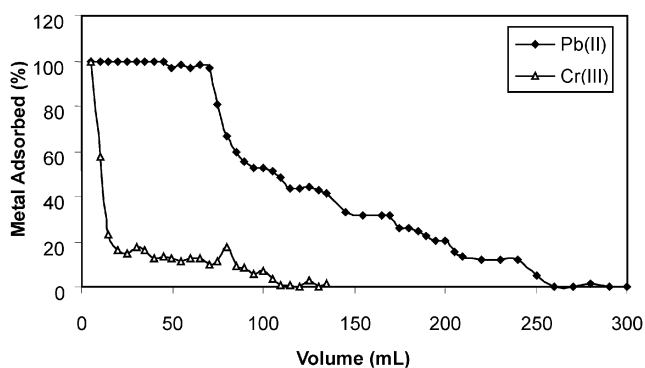


Fig. 5. Percentage of Pb(II) and Cr(III) adsorbed by CMPCR.

fractions (70 mL). This fact showed that CMPCR can be a good adsorbent for Pb(II). In the next fractions, percent of Pb(II) adsorbed decreased until the column was exhausted, i.e. when the effluent concentration equals to influent concentration. This exhausted column took place in the 50<sup>th</sup> fraction (250 mL), but the throughput volume applied to the column was 300 mL. In an other case, the amount of Cr(III) adsorbed at the first fraction (5 mL) was 100%, but in the next fractions, percent of Cr(III) adsorbed lessened until the column was exhausted which occurred in the 22<sup>nd</sup> fraction or 110 mL; meanwhile, the throughput volume applied to the column was 135 mL.

The breakthrough curve of Pb(II) adsorption is presented in Fig. 6. It can be seen that a 5% breakthrough point (BT), 50% BT, and a 100% BT occurred after passing of the feeding solution of about 70, 110 and 250 mL or about 58 bed volume (BV), 92 BV, and 208 BV, respectively. Shorter breakthrough points took place in the Cr(III) case wherein 5% BT, 50% BT, and 100% BT occurred after the feeding solution reached up to 5, 12, and 110 mL or about 4, 10 and 17.3 BV, respectively.

The column test also showed that the total uptake of Pb(II) ( $q_e$ ) was 4.166 mg Pb(II) per g of CMPCR, or 20.11  $\mu\text{mol/g}$  (Fig. 7). This value of adsorption column capacity

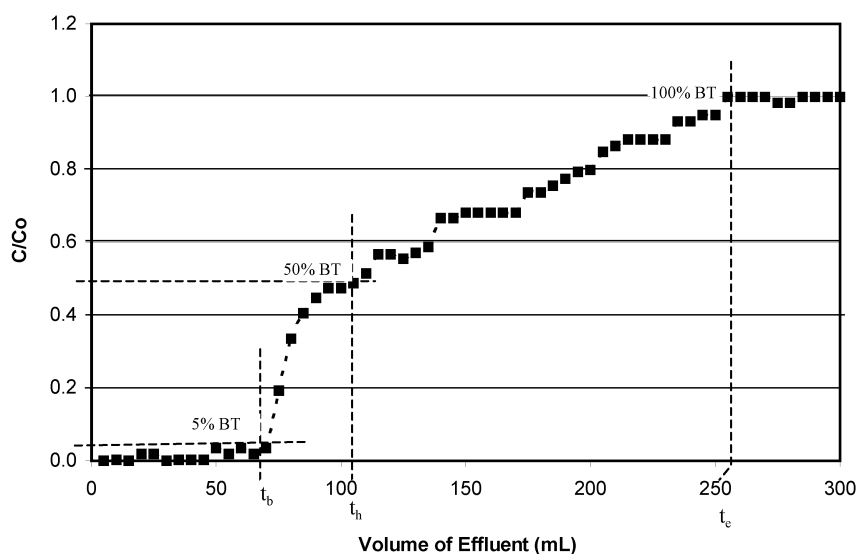


Fig. 6. Breakthrough curve of Pb(II) adsorption by CMPCR ( $C_0$  = initial metal ion concentration,  $C$  = metal ion concentration in the effluent).

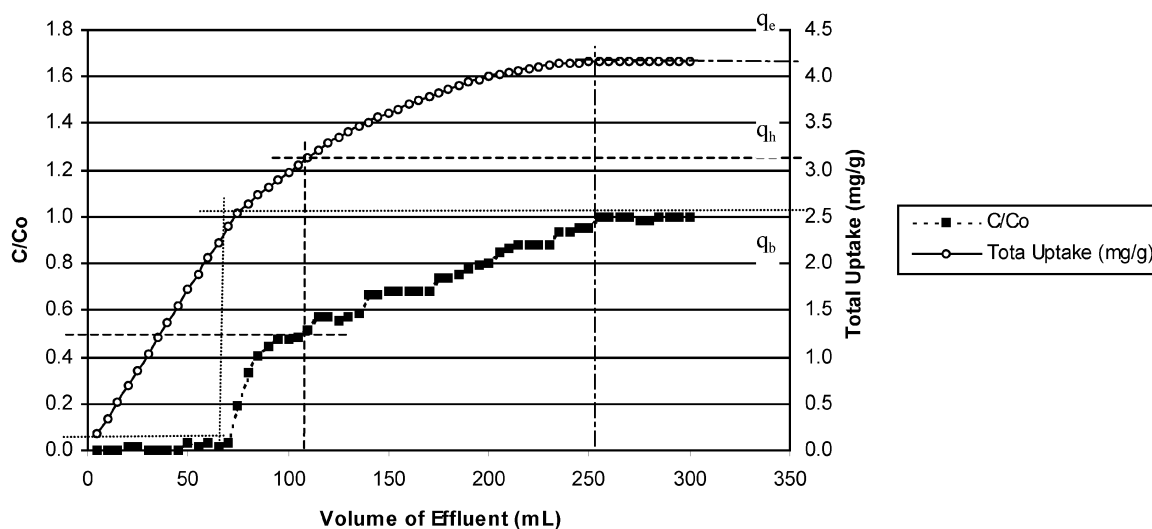


Fig. 7. The total uptake of Pb(II) adsorption.

was significantly higher compared to the value of adsorption capacity in a batch system that has a maximum capacity of about 0.85 mg/g or 4.1  $\mu\text{mol/g}$ . The initial breakthrough occurred at column loading of about 2.6 mg/g ( $q_b$ ). This means that the amount of Pb(II) adsorbed has reached 63% of the total uptake, although the Pb(II) solution applied was only 26% of total volume, or 74% of the operating cost would be consumed for taking 37% of the rest of Pb(II). Likewise, at  $C/C_0 = 0.5$ , the amount of Pb(II) adsorbed reached almost 77%, i.e. 3.2 mg/g, and consumed as much as 36% of the operating cost.

The curve in Fig. 8 shows that the total uptake of Cr(III) ( $q_e$ ) was 0.895 mg/g or 17.21  $\mu\text{mol/g}$ . Similar to Pb(II), the value of Cr(III) adsorption column capacity was significantly higher compared to the value of adsorption capacity in a batch system that has a maximum capacity of about 0.61 mg/g or 11.6  $\mu\text{mol/g}$ . The initial breakthrough occurred at column loading of about 0.22 mg/g ( $q_b$ ) or 24.7% of total uptake, and Cr(III) solution applied was 3.7% of total volume. At  $C/C_0 = 0.5$ , the amount of Cr(III) adsorbed reached almost 45.8%, i.e. 0.41 mg/g, and consumed as much as 8.8% of the operating cost. This means that 91.2% operating cost would be consumed for taking 54.2% of the rest of Cr(III). The results clearly showed that running a column as long as 8.8% of the throughput volume (or about 12 mL) was more efficient than running the column until exhaustion.

Fig. 9 presents breakthrough curves and uptakes of Pb(II) and Cr(III). The figure shows that Pb(II) and Cr(III) adsorptions have almost the same shape, but the former has quite a spread shape. Pb(II) curve has a breakthrough point ( $t_b$ ) which was significantly bigger than Cr(III), i.e.  $t_b$  of

Pb(II) was 160 minutes (66 BV) and  $t_b$  of Cr(III) was 10 minutes (8 BV). Similar to the exhaustion point ( $t_e$ ), Pb(II) has significantly longer  $t_e$  than Cr(III), i.e.  $t_e$  of Pb(II) was 500 minutes (208 BV) and  $t_e$  of Cr(III) was 220 minutes (almost 92 BV). A big breakthrough point was desired, but a big exhaustion point was not expected. A big breakthrough point means the amount of metal adsorbed is fairly high, but a big exhaustion point means high operational cost.

The total metal uptake of both Pb(II) and Cr(III) experiments showed different values, i.e. Pb(II) was 4.166 mg/g, whereas Cr(III) was only 0.89 mg/g. However, if the metal uptake values were expressed in mol/g, then these values were almost the same, i.e. Pb(II) was 20.11  $\mu\text{mol/g}$ , and Cr(III) was 17.21  $\mu\text{mol/g}$ . Therefore, it can be said that CMPCR adsorbed Pb(II) better than Cr(III), although the adsorption consumed more operational costs.

The breakthrough curve was used to calculate the length of unused bed ( $H_{UNB}$ ), the length of used bed ( $H_U$ ), and the overall mass-transfer coefficient ( $K_{ca}$ ).<sup>6,20</sup> Table 4

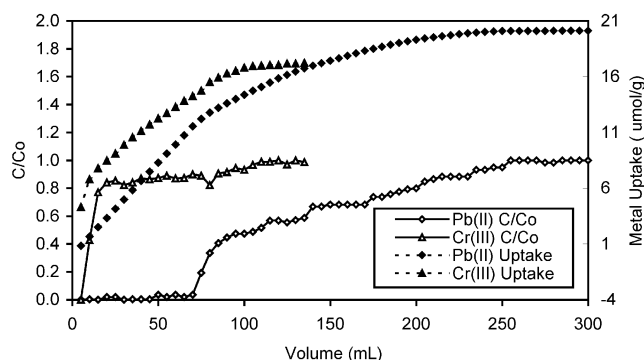


Fig. 9. Comparison of breakthrough curve and metal uptake between Pb(II) and Cr(III).

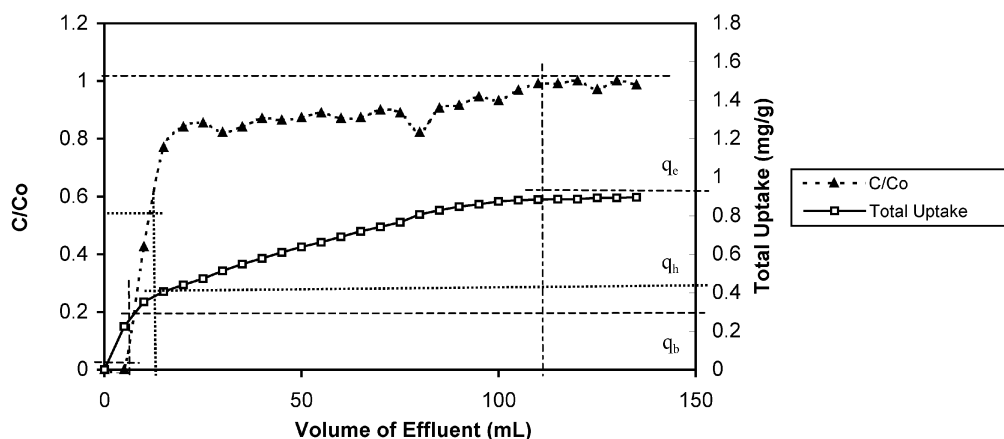


Fig. 8. The total uptake of Cr(III) adsorption.

Table 4. The breakthrough data and mass transfer parameters of Pb(II) and Cr(III) adsorptions

Parameter	Pb(II)	Cr(III)
$t_b$ (breakthrough point)	160 min	10 min
$t_e$ (exhausted point)	500 min	220 min
$H_{UNB}$ (the length of unused bed)	1.63 cm (68%)	2.28 cm (95%)
$H_U$ (the length of used bed)	0.77 cm (32%)	0.12 cm (5%)
$K_{ca}$ (the mass-transfer coefficient)	1.22 min <sup>-1</sup>	0.88 min <sup>-1</sup>

shows that  $H_{UNB}$  on Cr(III) adsorption was longer than on Pb(II). In the design of an adsorption column, it is important to minimize the length of the unused bed ( $H_{UNB}$ ). This length represents the length of mass-transfer zone, which is the part of the column where adsorbent is not completely used, but adsorption is still occurring. On the contrary, the length of used bed ( $H_U$ ) represents the part of the column in which adsorbent is completely saturated by adsorbate. Therefore, at this point, Pb(II) adsorption was better than Cr(III), because it has minimum  $H_{UNB}$ . A similar matter was observed at the overall mass-transfer coefficient ( $K_{ca}$ ). Adsorption of Pb(II) has higher  $K_{ca}$  than Cr(III) adsorption, thus, CMPCR was more appropriate to remove Pb(II) than Cr(III).

Table 5 presents the parameters of the Thomas model,<sup>20</sup> which were calculated by linear regression. The linearised Thomas equation did not describe the breakthrough data very well since the values of  $R^2$  were not very good, especially for Cr(III) adsorption. The Thomas rate constant ( $k$ ) of Pb(II) adsorption was slightly bigger than that of Cr(III). It was interesting to compare the maximum capacity of bed according to the Thomas model and the experimental result, since those values were fit enough. Based on the data at this point, the Thomas model can be considered as the appropriate model for the adsorption.

### Kinetic Aspect

The results of the kinetics studies on the adsorption of Pb(II) and Cr(III) are shown in Fig. 10. The time needed to reach equilibrium for Pb(II) adsorption was about 250 minutes (4.16 hours), which was longer than that required in the batch system (180 minutes). On the other hand, the time needed to reach equilibrium for Cr(III) adsorption was about 110 minutes (1.83 hours), which was shorter than that required in the batch system (360 minutes).

According to the graph, the kinetics of Pb(II) and

Table 5. The Thomas model parameters of Pb(II) and Cr(III) adsorptions

Parameter	Pb(II)	Cr(III)
The coefficient of correlation ( $R^2$ )	0.954	0.650
The rate constant ( $k$ , mg <sup>-1</sup> min <sup>-1</sup> )	0.485	0.459
The maximum capacity according to the Thomas model ( $X_m$ ; mg/g)	3.935	1.177
The maximum capacity according to experiment result ( $q_e$ ; mg/g)	4.166	0.895

Cr(III) adsorptions present a shape characterized by strong capacity adsorption during the first few minutes of contact, followed by slow increase until a state of equilibrium was reached. As an approximation, the removal of cations can be said to take place in two distinct steps: a relatively fast phase followed by a slower one.

Kinetics of heavy metal adsorption can be modeled by the first order Lagergren equation, the pseudo second order rate equation, and the second order rate equation. The results of linear plots of  $\log(q_e - q_t)$  versus  $t$ ,  $t/q_t$  versus  $t$ , and  $1/(q_e - q_t)$  versus  $t$  are shown in Table 6. The rate constant ( $k$ ) values can be calculated from the slopes or intercepts according to its equation. According to the data in the Table, the pseudo second-order reaction rate model adequately

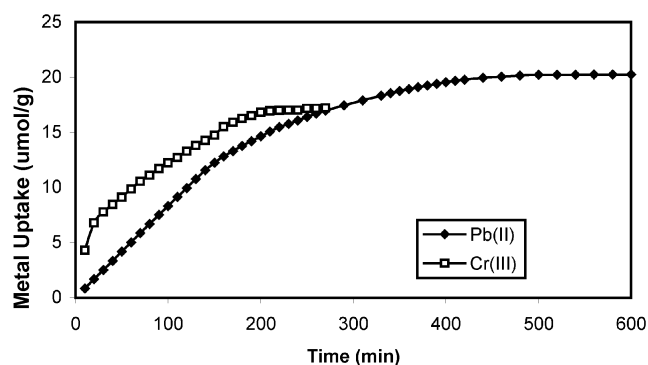


Fig. 10. Kinetics of Pb(II) and Cr(III) adsorptions.

Table 6. Kinetics parameters for Pb(II) and Cr(III) adsorptions

Reaction Rate Model	Pb(II)		Cr(III)	
	R <sup>2</sup>	k	R <sup>2</sup>	k
1 <sup>st</sup> order	0.9026	$1.95 \times 10^{-3} \text{ min}^{-1}$	0.9229	$3.90 \times 10^{-3} \text{ min}^{-1}$
Pseudo 2 <sup>nd</sup> order	0.9569	$6.97 \times 10^{-4} \text{ g mmol}^{-1} \text{ min}^{-1}$	0.9695	$1.28 \times 10^{-2} \text{ g mmol}^{-1} \text{ min}^{-1}$
2 <sup>nd</sup> order	0.3452	$2.62 \times 10^{-1} \text{ g mmol}^{-1} \text{ min}^{-1}$	0.4479	$7.76 \times 10^{-1} \text{ g mmol}^{-1} \text{ min}^{-1}$

described the kinetics of both Pb(II) and Cr(III) adsorptions with the highest correlation coefficient. Therefore, it was possible that both adsorbent and adsorbate gave contribution to the reaction rate. Nevertheless, the rate adsorption constants of a fixed bed column system appeared in contrary performance compared to the batch system. In the fixed bed column system, the rate constant of Pb(II) was lower than that of Cr(III), thus it could be considered that Pb(II) adsorption ran slower than Cr(III).

### Desorption

A desorption test was done sequentially to leach heavy metal cations which have been adsorbed onto CMPCR. This experiment was conducted to recover the column and to estimate the types of adsorption mechanisms, hence different solutions was eluted to the column. The principle of this model is the usage of different desorption agents which have a desorption ability that increased sequentially, i.e. (1) desorption by water to confirm the adsorption mechanism physically (entrapment), (2) desorption by acid solution (HCl), which was used to leach metal cations adsorbed by chemical adsorption via ion exchange or hydrogen bond mechanism.

The result of Pb(II) desorption is performed in Fig. 11. According to the graph, water leached Pb(II) poorly, only about 4.61%, whereas 1 M HCl solution leached Pb(II) completely, up to 99.24%. Based on the data, Pb(II) adsorption by CMPCR was dominated by chemisorption (more than 95%); on the contrary, physisorption ruled the adsorption mechanism in a small portion (less than 5%).

Fig. 12 depicts the result of Cr(III) desorption. According to the graph, the elution tendency as percentage recovery of Cr(III) followed the sequence: distilled H<sub>2</sub>O (1.7%) < 0.1 M HCl (98.12%). Water acted very poor as a Cr(III) desorption agent, whereas 0.1 M HCl solution was an excellent Cr(III) desorption agent. Similar to Pb(II) adsorption, Cr(III) adsorption was dominated by chemisorp-

tion (more than 98%). Most Pb(II) and Cr(III) adsorbed onto CMPCR were estimated via ionic and hydrogen bonding mechanism.

## EXPERIMENTAL SECTION

### Reagents

Metal solutions were prepared by diluting 1000 mg/L Pb(NO<sub>3</sub>)<sub>2</sub> and Cr(NO<sub>3</sub>)<sub>3</sub> standard solution in aqueous nitric acid to desired concentrations. An adjustment of pH was carried out by adding slowly NaOH and/or HNO<sub>3</sub> solution(s) into the metal solutions followed by stirring until the desired pH was reached. Chemicals needed for synthesizing CMPCR were resorcinol, 4-methoxybenzaldehyde, HCl, and ethanol. All materials required were reagent grade from E Merck.

### Instruments

In this experiment, equipment involving a set of reflux utilities, Buchner funnels, <sup>1</sup>H and <sup>13</sup>C NMR spectrom-

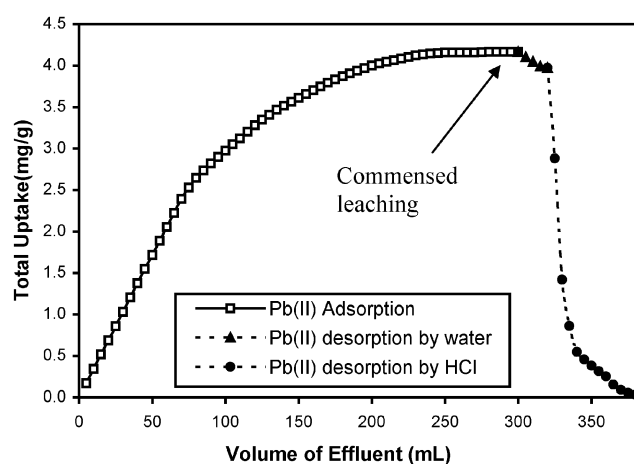


Fig. 11. Sequential desorption of Pb(II) by water and HCl 1 M.

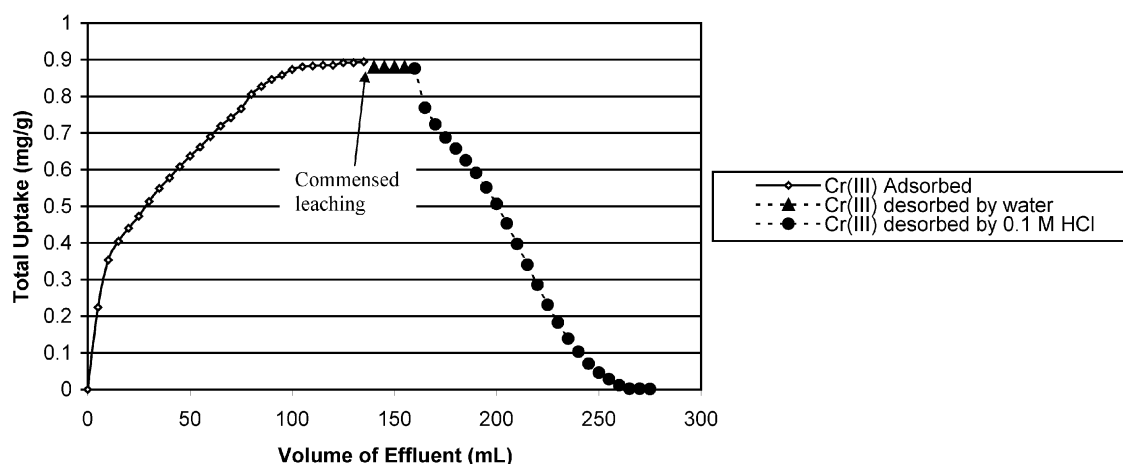


Fig. 12. Sequential desorption of Cr(III) by water and 0.1 M HCl.

eter (Jeol JNM-AL300 FT NMR System, 300 MHz), and FTIR spectrophotometer (Shimadzu FTIR 8201PC) were used for CMPCR synthesizing and characterization. Pump, glass column, stirrer, Atomic Absorption Spectrophotometer (AAS; Perkin Elmer Analyst-100), and pH meter (Hanna), were used for adsorption experiment and determination of Pb(II) and Cr(III) concentrations.

### Synthesis of CMPCR

Into a solution of resorcinol (2.2 g, 0.02 mol) and 4-methoxybenzaldehyde (2.72 g, 0.02 mol) in 20 mL of 95% ethanol was added 4 mL of hydrochloric acid. The solution was stirred and refluxed at 78 °C for 24 hours. The product that separated was filtered. The solid was washed using ethanol-water repeatedly and then dried to give the desired compound as a light purple solid in 85.7% (3.91 g): mp > 390 °C (dec), <sup>1</sup>H NMR (300 MHz, 298 K, DMSO, TMS) δ<sub>H</sub>: C<sub>2v</sub> isomer: 3.63 (12H, s, OCH<sub>3</sub>), 5.45 (4H, s, CH), 6.11-6.62 (24H, m, ArH), 8.44 (4H, s, ArOH), 8.46 (4H, s, ArOH); C<sub>4v</sub> isomer: 3.69 (18H, s, OCH<sub>3</sub>), 5.57 (6H, s, CH), 6.11-6.62 (36H, m, ArH), 8.46 (12H, s, ArOH).

### Adsorption Procedures

A batch experiment was conducted by adding 0.1 g of CMPCR (its particle size was < 100 mesh) into 10 mL of metal cation sample solution having a concentration of 8 mg/L. The mixture was shaken at room temperature for a certain period of time. The adsorbent was filtered out and dried in a desiccator. Concentration of metal ion was then measured by AAS. The data obtained was compared and

corrected by a blank solution. The blank solution was similar to the adsorption sample except for the existence of the adsorbent. The amount of metal cation adsorbed was calculated from the difference between the metal cation concentration before and after the adsorption experiment. The metal uptake, *q* (mg metal ion/g CMPCR) was determined as follows:

$$q = (C_0 - C) \times V/m \quad (1)$$

where *C*<sub>0</sub> and *C* are the initial and the final metal ion concentrations (mg/L), respectively; *V* is the volume of solution (mL); and *m* is the CMPCR weight (g) in dry form. For each metal cation, the experiment was done in 3 conditions, i.e. variation of pH, shaking time, and adsorbent weight.

The fixed bed column adsorption experiment was done in a descendant flow. The equipment used is depicted in Fig. 13. The metal solutions were prepared by diluting 1000 mg/L metal cation standard solution in aqueous nitric acid to the desired concentration. Adjustment of pH of the metal solutions was carried out by adding slowly NaOH and/or HNO<sub>3</sub> solutions followed by stirring until the desired pH was reached. This metal solution was passed through the column in a down flow at a fixed flow rate. The solution which passed through the column was fractionated into 5 cm<sup>3</sup> portions, and the effluent concentration was determined by AAS. Fractions of the effluent were collected until the ratio of effluent concentration (*C*) to initial concentration (*C*<sub>0</sub>) equals to one.

The ratio of *C*/*C*<sub>0</sub> called as breakthrough was plotted

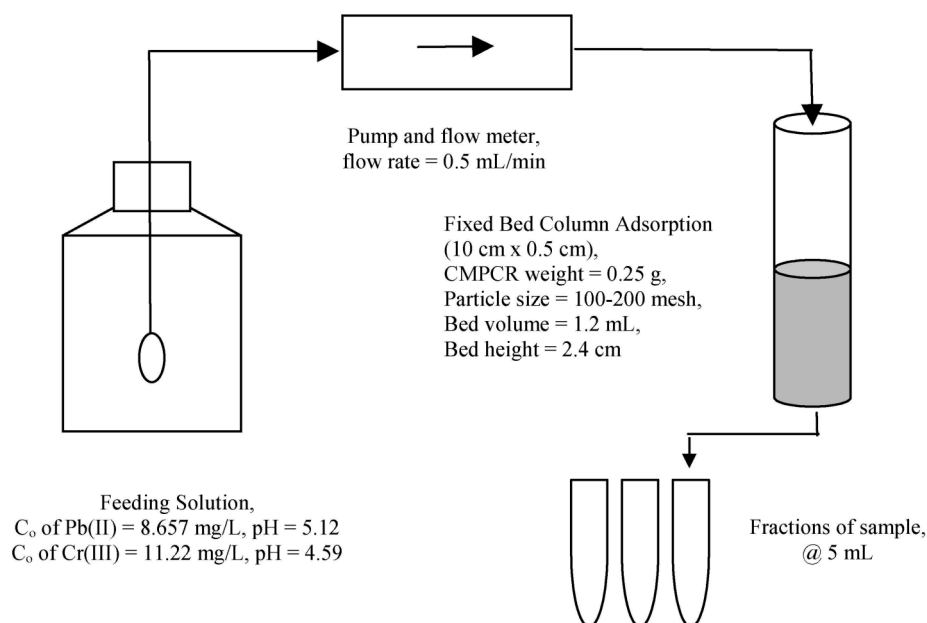


Fig. 13. Apparatus for fixed bed column adsorption experiment.

against the volume of the solution passed in the column or against the time to obtain a breakthrough curve. The breakthrough time,  $t_b$ , was determined as the time when  $C/C_o$  was equal to 0.05. Based on the breakthrough curve, the length of unused bed ( $H_{USB}$ ), the length of used bed ( $H_U$ ), the overall mass-transfer coefficient ( $K_{ca}$ ), the Thomas rate constant ( $k$ ), and the maximum capacity of the bed according to the Thomas model ( $X_m$ ) were then calculated.<sup>6,20</sup>

Desorption process was done sequentially. Metal adsorbed was eluted with water, followed by aqueous HCl solution at the desired flow rate, and 5 mL of fractions were collected. Elution for each desorption agent was conducted until the effluent metal concentration equals the influent metal concentration.

#### ACKNOWLEDGEMENT

The authors deeply thank the State Ministry for Research and Technology of the Republic of Indonesia for providing financial support for this research through its International Joint Research Program (RUTI).

Received November 10, 2006.

#### REFERENCES

1. Igwe, J. C.; Ogunewe, D. N.; Abia, A. A. *Afr. J. Biotechnol.* **2005**, *10*, 1113-1116.
2. Izanloo, H.; Nasseri, S. *Iranian J. Env. Health Sci. Eng.* **2005**, *2*, 33-42.
3. Qadeer, R. *J. Zhejiang Univ. SCI* **2005**, *5*, 353-356.
4. Li, Z.; Sun, X.; Luo, J.; Hwang, J.-Y. *J. Min. & Mat. Char. & Eng.* **2002**, *1*, 79-96.
5. Barros, M. A. S. D.; Zola, A. S.; Arroyo, P. A.; Sousa-Agular, E. F.; Tavares, C. R. G. *Acta Scientiarum* **2002**, *6*, 1619-1625.
6. Barros, M. A. S. D.; Zola, A. S.; Arroyo, P. A.; Sousa-Agular, E. F.; Tavares, C. R. G. *Braz. J. Chem. Eng.* **2003**, *20*, 4.
7. Dianati-Tilaki, R. A.; Mahmood, S. *Pak. J. Biol. Sci.* **2004**, *5*, 865-869.
8. Britz-Mckibbin, P.; Chen, D. D. Y. *Anal. Chem.* **1998**, *70*, 907-912.
9. Jain, V. K.; Pillai, S. G.; Pandya, R. A.; Agrawal, Y. K.; Shrivastav, P. S. *Anal. Sci.* **2005**, *21*, 129-135.
10. Mustafina, A. R.; Skripacheva, V. V.; Fedorenko, S. V.; Kazakova, E. K.; Konovalov, A. I. *Butlerov Comm.* **2000**, *3*.
11. Wei, A.; Kim, B.; Pusztay, S. V.; Tripp, S. L.; Balasubramanian, R. *J. Incl. Phen & Macrocyc. Chem.* **2001**, *41*, 83-86.
12. Pietraszkiewicz, M.; Pietraszkiewicz, O.; Uzig, E.; Prus, P.; Brzozka, Z.; Woniak, K.; Bilewicz, R.; Borowiaak, T.; Czysnki, M. M. *Butlerov Comm.* **2000**, *3*. Available on website at <http://chem.kstu.ru/JCHEM&CS/English/n3/sm3/sm3.htm>

13. Barrett, A. G.; Braddock, D. C.; Henschke, J. P.; Waalker, E. R. *J. Chem. Soc., Perkin Trans I* **1999**, 873-878.
14. Tunstad, L. M.; Tucker, J. A.; Daicanale, E.; Weiser, J.; Bryant, J. A.; Sherman, J. C.; Helgeson, R. C.; Knobler, C. B.; Cram, D. J. *J. Org. Chem.* **1989**, *54*, 1305-1312.
15. Roberts, B. A.; Cave, G. W. V.; Raston, C. L.; Scott, J. L. *Green Chem.* **2001**, *3*, 280-284.
16. Yamakawa, Y.; Ueda, M.; Nagahata, R.; Takeuchi, K.; Asai, M. *J. Chem. Soc., Perkin Trans I* **1998**, 4135-4139.
17. Manna, B.; Dasgupta, M.; Ghosh, U. C. *J. Water Supply: Res. & Tech-AQUA* **2004**, *7*, 483-495.
18. Tofan, L.; Paduraru, C. *Croat. Chem. Acta* **2004**, *4*, 581-586.
19. Goswami, S.; Ghosh, U. C. *Water SA* **2005**, *31*, 597-602.
20. Mantovaneli, I. C. C.; Ferretti, E. C.; Simoes, M. R.; da Silva, F. *Braz. J. Chem. Eng.* **2004**, *21*, 449-458.